On The Development of Parameterized Linear Analytical Longitudinal Airship Models

Eric A. Kulczycki*
NASA Jet Propulsion Laboratory, Pasadena, California, 91109

Joseph R. Johnson†
Clemson University, Clemson, SC, 29631

David S. Bayard‡
NASA Jet Propulsion Laboratory, Pasadena, California, 91109

Alberto Elfes§
NASA Jet Propulsion Laboratory, Pasadena, California, 91109

and

Marco B. Quadrelli**
NASA Jet Propulsion Laboratory, Pasadena, California, 91109

In order to explore Titan, a moon of Saturn, airships must be able to traverse the atmosphere autonomously. To achieve this, an accurate model and accurate control of the vehicle must be developed so that it is understood how the airship will react to specific sets of control inputs. This paper explains how longitudinal aircraft stability derivatives can be used with airship parameters to create a linear model of the airship solely by combining geometric and aerodynamic airship data. This method does not require system identification of the vehicle. All of the required data can be derived from computational fluid dynamics and wind tunnel testing. This alternate method of developing dynamic airship models will reduce time and cost. Results are compared to other stable airship dynamic models to validate the methods. Future work will address a lateral airship model using the same methods.

Nomenclature

$a_{aircraft}$	=	aircraft *a* matrix with masses
$a_{airship}$	=	airship *a* matrix with masses
a, b	=	Semi-major and semi-minor axis of an ellipsoid (m)
a_x, a_z	=	Center of Gravity Coordinates With Respect to Center Of Volume (m) in body frame
b_x, b_z	=	Center of Buoyancy Coordinates With Respect to Center Of Volume (m) in body frame

*Member of Technical Staff, NASA Jet Propulsion Laboratory, California Institute of Technology, Pasadena, California 91109
†Research Assistant, Department of Mechanical Engineering, Flour Daniel, Clemson University, Clemson, South Carolina, 29632
‡Principal Member of Technical Staff, NASA Jet Propulsion Laboratory, California Institute of Technology, Pasadena, California 91109
§Principal Member of Technical Staff, NASA Jet Propulsion Laboratory, California Institute of Technology, Pasadena, California 91109
**Senior Member of Technical Staff, NASA Jet Propulsion Laboratory, California Institute of Technology, Pasadena, California 91109

$\bar{c}$	=	Mean Aerodynamic Chord (m)
d	=	Diameter of largest cross section of airship (m)
d_x, d_y, d_z	=	X, Y, and Z distances between the line connecting the two engines thrust lines and the OZ axis, OXZ plane, and OXY plane, respectively (m) in body frame
e	=	Eccentricity
$f_i,$	=	Forces contributing to Coriolis effects (N)
g	=	Acceleration Due to Gravity (m/s^2)
k_1, k_2, k'	=	Lamb's inertia ratios for movement along OX, OY and rotation about OY
l	=	Length of airship (m)
l_t	=	Tail moment arm (m)
m	=	Mass of airship (kg)
$m_{aircraft}$	=	Mass matrix of aircraft
$m_{airship}$	=	Mass matrix of airship
m_x, m_y, m_z	=	Apparent Masses (kg)
p, q, r	=	Airship Angular Velocities about the X, Y, and Z axis (rad/s)
$\dot{p}, \dot{q}, \dot{r}$	=	Airship Angular Accelerations about the X, Y, and Z axis (rad/s^2)
$\bar{u}$	=	Control Input Vector
u, v, w	=	Airship Translational Velocities in the X, Y, and Z directions (m/s)
$\dot{u}, \dot{v}, \dot{w}$	=	Airship Translational Accelerations in the X, Y, and Z directions (m/s^2)
$\bar{x}$	=	State Vector
A	=	Aerodynamic Force Vector
$A_{4\times4}$	=	A Matrix for State-Space Representation
$A_{aircraft}$	=	Aircraft A matrix without mass terms
$A_{airship}$	=	Airship A matrix without mass terms
A_X, A_Y, A_Z	=	Aerodynamic Total Force about OX, OY, and OZ axes (N)
A_L, A_M, A_N	=	Aerodynamic Total Moment about OX, OY, and OZ axes (N)
B	=	Buoyancy Force Acting at the Center of Volume (N)
$B_{4\times2}$	=	B Matrix for State-Space Representation
C_{D_0}	=	Zero-lift drag Coefficient
C_{D_α}	=	Coefficient of the change in drag w.r.t. angle of attack
C_{D_u}	=	Coefficient of the change in drag w.r.t. forward velocity u
C_L	=	Coefficient of lift
C_{L_0}	=	Coefficient of lift at zero angle of attack
C_{L_α}	=	Coefficient of the change in lift w.r.t. angle of attack
$C_{L_{\alpha_t}}$	=	Coefficient of the change in lift w.r.t. tail angle of attack
C_{L_u}	=	Coefficient of the change in lift w.r.t. forward velocity u
C_{M_α}	=	Coefficient of pitching moment w.r.t. angle of attack
$C_{M_{\delta_e}}$	=	Coefficient of pitching moment w.r.t. elevator angle

C_{M_q} = Coefficient of change in pitching moment w.r.t. pitching velocity q

C_{M_u} = Coefficient of change in pitching moment w.r.t. forward velocity u

$C_{Z_{\delta_e}}$ = Coefficient of change in normal force w.r.t. elevator angle

C_{Z_q} = Coefficient of change in normal force w.r.t. pitching velocity q

F_d = Dynamic Force vector

G = Gravitational and Buoyant Force vector

I_x, I_y, I_z = Moments of Inertia about the X, Y, Z axes (kg·m^2)

I_{xy}, I_{xz}, I_{yz} = Products of Inertia about OX, OY, OZ (kg·m^2)

J_x, J_y, J_z = Apparent Moments of Inertia about the X, Y, Z axes (kg·m^2)

J_{xy}, J_{xz}, J_{yz} = Apparent Products of Inertia about OZ, OY, and OX (kg·m^2)

$\mathring{L}_{\dot{p}}, \mathring{L}_{\dot{r}}, \mathring{L}_{\dot{v}}, \mathring{M}_{\dot{u}}\ \mathring{M}_{\dot{q}}, \mathring{M}_{\dot{p}}, \mathring{M}_{\dot{w}}, \mathring{N}_{\dot{r}}, \mathring{N}_{\dot{q}}, \mathring{N}_{\dot{v}}$ = Virtual Inertia Terms (kg·m^2)

M = Mass Matrix

M_a = Mach number

M_e = Trim pitching moment (N·m)

$\mathring{M}_u$ = Change in pitching moment w.r.t. forward velocity u (1/ (m·s))

$\mathring{M}_w$ = Change in pitching moment w.r.t. vertical velocity w (1/ (m·s))

$\mathring{M}_q$ = Change in pitching moment w.r.t. pitching velocity q (1/s)

$\mathring{M}_{\delta_e}$ = Change in pitching moment w.r.t. change in elevator angle (1/s^2)

$\mathring{M}_{\delta_t}$ = Change in pitching moment w.r.t. change in thrust (1/s^2)

P = Propulsion Force Vector

Q = Flight dynamic pressure (N/m^2)

S = Surface area of lifting surface (m^2)

S_t = Tail surface area (m^2)

T_e = Trim equilibrium thrust (N)

T_s, T_p, T_0 = Starboard, Port, and Total thrusts (N)

U_e, W_e = Trim velocities in the X and Z direction (m/s)

$\dot{U}, \dot{V}, \dot{W}$ = Linear Translational Axial, Side, and Normal Acceleration Perturbations (m/s^2)

V_H = Horizontal tail volume ratio

Vol = Volume of airship (m^3)

W = Weight of Airship Acting at the Center of Mass (N)

$\mathring{X}_u$ = Change in X force w.r.t. forward velocity u (1/s)

$\mathring{X}_w$ = Change in X force w.r.t. vertical velocity w (1/s)

$\mathring{X}_q$ = Change in X force w.r.t. pitching velocity q (1/s)

$\mathring{X}_{\delta_e}$ = Change in X force w.r.t. change in elevator angle (1/s)

$\mathring{X}_{\delta_t}$ = Change in X force w.r.t. change in thrust (1/s)

X, Y, Z = Axial, Side and Normal Forces (N)

X_e, Y_e, Z_e = Trim axial aerodynamic force in the X, Y, and Z directions (N)

$\mathring{X}_{\dot{u}}, \mathring{X}_{\dot{q}}, \mathring{Y}_{\dot{v}}, \mathring{Y}_{\dot{r}}, \mathring{Y}_{\dot{p}}, \mathring{Z}_{\dot{w}}, \mathring{Z}_{\dot{q}}$ = Virtual Masses (kg)

$\mathring{Z}_u$ = Change in Z force w.r.t forward velocity u (1/s)

$\mathring{Z}_w$ = Change in Z force w.r.t. vertical velocity w (1/s)

$\mathring{Z}_q$ = Change in Z force w.r.t. pitching velocity q (1/s)

$\mathring{Z}_{\delta_e}$ = Change in Z force w.r.t. change in elevator angle (1/s)

$\mathring{Z}_{\delta_t}$ = Change in Z force w.r.t. change in thrust (1/s)

$\overline{\alpha}, \overline{\beta}$ = Numerical calculations for Lamb's constants

$\delta_e, \delta_r, \delta_t$ = Elevator, Rudder, and Tail Surface Deflection Angles (rad)

λ_{ij} = Elements of the Directional Cosine Matrix

η = Tail efficiency

ρ = Density of surrounding air (kg/m^3)

θ, ϕ, ψ = Pitch, Roll, and Yaw Angles of Airship (rad)

θ_e = Trim pitch angle (rad)

τ = Flap effectiveness

μ_s, μ_p = Starboard and Port Thrust Angle (rad)

I. Introduction

THE search for inhabitable planets that have the capability to sustain life is a major element that drives space exploration. There are two Mars Exploration Rovers (MER) currently active on the surface of Mars (Spirit and Opportunity) with a third rover under development, the Mars Science Laboratory (MSL) rover. All of these robotic systems have the goal of determining if water exists or existed on the surface since its presence is usually indicative of life. Another celestial body that has similar characteristics to Earth and could potentially support life is Titan, a moon of Saturn. Titan is significantly further from Earth than Mars, increasing the difficulty, cost, and time that will have to be spent to send a mission to its surface. It is very important that any robotic system sent there is able to explore as much of the planet as possible.

On Titan there are two mediums by which a vehicle could travel: ground and air. Currently, there is more experience and information on lander and rover technology. Landers provide high-resolution data and results from on-board science tools, but only for a single site. Rovers provide similar information, but are able to move from site to site based on scientific interest in the 2D world. These ground-based explorers return valuable data, but are limited by the distancd they can travel. Aerial systems can utilize the wind fields and minimize the energy needed to explore greater distances and areas that a rover or lander cannot reach. In addition, Titan's surface temperature is estimated to be 93°K which would require a rover to traverse complex icy terrain, which is a very significant challenge for current rover systems. Titan has a high atmospheric density of 5.3 kg/m^3 at low altitudes which is almost 4.5 times that of Earth. This dense atmosphere enables aerial travel and allows aerial vehicles to carry science instrument payloads of significant size.

Of the feasible air vehicles, such as airplanes, gliders, balloons, helicopters and airships[7], only a few meet the necessary criteria to operate on Titan. Due to the 2.6 hour communication delay between Earth and Titan, the aerial vehicle will require a large amount of autonomy to stay aloft while awaiting subsequent commands. For vehicles

such as powered fixed-wing aircraft and gliders, high speeds need to be maintained to continue flight, resulting in continuous forward movement. This is challenging because the position of the vehicle is constantly changing while it is waiting for commands from Earth. Hovering is advantageous in this respect, which helicopters, airships, and balloons can all achieve. However, helium-filled balloons have no position or orientation control and are taken wherever the winds lead them. Montgolfiere (Hot-Air) balloons are limited in their maneuverability by only having vertical velocity and altitude control. Montgolfiere balloons rely on using wind fields for navigation, but still lack the orientation control seen in airships[15]. However, in the powered flight comparison of helicopters and aircraft to airships, helicopters and aircraft expend significantly more energy maintaining flight. Consequently, the low power requirement for level flight is the key reason airships are often proposed as the best method for Titan exploration[2].

Autonomous airship control requires a good understanding of the vehicle's dynamics. There are many parameters in a nonlinear airship dynamic model that are unique to lighter-than-air vehicles and are difficult to estimate, such as buoyant forces, virtual mass, and inertia terms. The development of linear dynamic airship models has always required either the use of numerical methods to linearize a mathematical nonlinear model, or extensive flight data to enable the use of system identification methods. The significance of the model described in this paper is that it relies on merging the estimation techniques for dynamic stability derivatives found in the aircraft literature[1] with the linearized dynamic equations of motion for an Airship[3]. This paper demonstrates that with a reliable estimate of the airship aerodynamics obtained using CFD software or wind tunnel testing, and an accurate geometric model, it is possible to develop a parameterized linear longitudinal airship dynamic model.

II. History of Airship Dynamic Modeling

The difficulty in modeling airships arises from the different geometries, compositions, and projected flight patterns that are not native to conventional aircraft. Airships are lighter-than-air aerial vehicles having unique properties that affect their dynamics including the effects of buoyant forces and the virtual mass and inertias. Additionally, the center of volume is far from the center of mass causing the system to act as a pendulum, oscillating unnecessarily if the system is not controlled properly. The variety of operations that the airship must perform also presents difficulties in creating a dynamic model of the ship, since it must be able to hover, take off/land, ascend/descend, perform high and low speed travel, and traverse long distances.

There is a history of research that addresses the problem of airship dynamic modeling to determine its stability. Stability derivatives were used to create linear equations to analyze the ZR-1 and ZR-4 heavy lifting airships, in both linear and nonlinear operating regimes[9 10]. In the nonlinear realm, a comprehensive study on stability in airships was performed on the YEZ-2A airship for set trim conditions[4]. Results using a linear model have also been achieved by using the ADAMS 12.0 modeling software which allows Simulink interface, animation, and automatic equation of motion implementation[2]. The Jet Propulsion Laboratory is also developing a nonlinear airship model based on using the Darts/DSENDS program[11].

Linear models of the airship have also been created. Tischler used onboard frequency sweeps to excite the airship, and recorded the resulting responses to model the airship[12]. A state space linearized longitudinal model was created by the AURORA team by estimating the aerodynamic coefficients and refining them with system identification. A detailed discussion on how the equations of motion for an airship are linearized is given in Cook, who adapted the mathematical model for a body submersed in fluid[3]. The method used was the small perturbations method, as detailed in Section IV.

III. JPL Titan Aerobot Program Background

A. Mission Background

The Titan Explorer mission, as outlined by the solar system exploration roadmap[6], is intended to take a closer look at Titan, and is proposed to be one of NASA's flagship missions during the second decade of the 21st century. The Titan aerobot will follow the Cassini and Huygens missions, building upon their observations. The mobility of the aerobot will allow for larger coverage areas, sub-haze layer exploration, collecting data on lower atmosphere winds, clouds, and precipitation, and in situ measurements of ices and organic materials at the surface to assess prebiotic/protobiotic chemistry. Obtaining the data from Titan would be performed in a fashion analogous to the acquisition of a sea floor sample by a submersible. The science goal for the mission would be the characterization of these organic and inorganic materials and determination of the origin of the diverse landforms identified in Huygens visual images and Cassini radar data.

The challenges in gathering data from Titan include the very cold temperatures (~ 93K) and long earth communication time which will demand special consideration for the design, material selection, mechanisms,

electronics, and advanced autonomy. While there are many challenges for this mission, an airship is well suited for the task due to Titan's high atmospheric density at the surface and the very low surface winds.

B. JPL Test Bed

The prototype aerobot test bed developed at the Jet Propulsion Laboratory (JPL) is based on an Airspeed Airship AS-800B, which can be seen below in Fig. 1. The airship specifications are: length of 11 m, diameter of 2.5 m, total volume of 34 m^3, two 2.3 kW (3 hp) 23 cm^3 (1.08 cubic inch) nitro methane fuel engines, double catenary gondola suspension, control surfaces in an "X" configuration, maximum speed of 13 m/s (25 kts), maximum ceiling of 500 m, average mission endurance of 60 minutes, static lift payload of 12 kg, and dynamic lift payload of up to 16 kg. The avionics and communication systems are installed in the gondola.

Figure 1: JPL Aerobot

The aerobot avionics system is built around a dual PC-104+ computer architecture. One of the PC-104+ stacks is used for navigation and flight control, while the other is dedicated to image processing. The navigation stack also has a serial board interface to the navigation sensors and pan/tilt unit, a timer/counter board for reading pulse width modulated (PWM) signals from a human safety pilot and generating PWM signals based upon control surface commands from the avoidance software, and an IEEE 1394 board for sending commands to, and reading image data from, the navigation and science cameras. The perception processor is dedicated to image processing and image-based motion estimation (IBME). Wireless serial modems provide data/control telemetry to the ground station. The safety pilot can always reassert "pilot override" control over the aerobot.

The navigation sensors currently consist of an Inertial Measurement Unit (IMU) which provides angular rates and linear accelerations, a compass/inclinometer which provides yaw, roll, and pitch angles, and a differential GPS (DGPS) for absolute 3D position. The vision sensors include two down-looking navigation cameras, one with a 360° x 180° field of view (FOV) and another with a narrower FOV. Additionally, we plan to integrate a laser altimeter (surface relative altitude), a barometric altimeter (absolute altitude against reference point), an ultrasonic anemometer (3D wind speed), and a science camera mounted on a pan/tilt unit.

The ground station is composed of a laptop, a graphics user interface to the vehicle, wireless data and video links, video monitors and VCRs, and a differential GPS (DGPS) base station that provides differential corrections to the GPS receiver onboard the aerobot. This provides vehicle 3D position estimates accurate to several centimeters. Field tests of the JPL aerobot are conducted at the Southern California Logistics Airport in Victorville, CA. Initial flights were teleoperated to allow extensive testing of the onboard avionics and data acquisition systems.[11]

C. Davis Model/Work

At the University of California at Davis, a nonlinear airship model has been created which builds upon many of the past airship models[14]. This model is comprised of parameterized physical elements, allowing for the model to easily accommodate the geometries and characteristics of other airships. These elements include the ellipsoidal hull, gondola, power unit, two vector thrusters, four tail rotors, and four fins. With this model, which was created in ADAMS software, UC Davis and JPL have conducted experiments investigating the effects of mass placement and sudden net-buoyancy changes on the behavior of flight controllability of the Titan aerobot[14].

D. Darts/Dsends work

To test the numerical models created at JPL, a simulation environment has been created for the Titan aerobot to use. This environment allows flight algorithms and control techniques to be tested before they are implemented on the physical airship, saving both money and time. The simulation has been validated under Earth conditions allowing it to then be used to predict the performance of JPL's airship on Titan. This environment is based on a spacecraft simulation created by the DARTS/Dshell tool[7]. The Dynamics Algorithms for Real-Time Simulation (DARTS) is a real-time flexible-body, mulitbody dynamics package developed at JPL. The Darts shell (Dshell) tool integrates reusable hardware and environmental models with the DARTS program. This aircraft simulator takes into account aerodynamics, mass properties, buoyancy, kinematics, dynamics, control surfaces, simulated sensors, terrain models, and much more. The models are parameterized to allow for varying airships to be tested, and the simulator

can determine model parameters through system identification. The simulation can be run with or without a GUI[13]. The model is also is the basis for the Dynamics Simulator for Entry Descent and Surface landing (DSENDS) entry, descent, and landing simulation[11].

IV. Airship Dynamics

This section will show how to develop an airship longitudinal analytical linearized model using a new approach called the Common "a" method. The process begins with the nonlinear equations of motion for an airship. The equations are linearized into longitudinal and lateral decoupled models. The longitudinal equations are arranged in state-space form, and then employ aircraft stability derivatives and reasonable assumptions to populate the longitudinal linear airship model equations, which creates a sound and stable linear longitudinal airship dynamic model.

A. Nonlinear Equations of Motion

This section describes the method used to create a nonlinear airship model beginning by defining the general mass and inertial properties of the airship. The method below is taken from Gomes' thesis[4] and the equations are taken from Khoury and Gillett's book *Airship Technology*[3].

1. Virtual mass effects

Axial force component $= \dfrac{\partial X}{\partial \dot{U}}\dot{U} \equiv \overset{\circ}{X}_{\dot{u}}\dot{U}$ (1)

Side force component $= \dfrac{\partial Y}{\partial \dot{V}}\dot{V} \equiv \overset{\circ}{Y}_{\dot{v}}\dot{V}$ (2)

Normal force component $= \dfrac{\partial Z}{\partial \dot{W}}\dot{W} \equiv \overset{\circ}{Z}_{\dot{w}}\dot{W}$ (3)

2. Components of apparent mass

$$m_x = m - \overset{\circ}{X}_{\dot{u}} \tag{4}$$

$$m_y = m - \overset{\circ}{Y}_{\dot{v}} \tag{5}$$

$$m_z = m - \overset{\circ}{Z}_{\dot{w}} \tag{6}$$

3. Apparent moments of inertia

$$J_x = I_x - \overset{\circ}{L}_{\dot{p}} \tag{7}$$

$$J_y = I_y - \overset{\circ}{M}_{\dot{q}} \tag{8}$$

$$J_z = I_z - \overset{\circ}{N}_{\dot{r}} \tag{9}$$

4. Apparent products of inertia

$$J_{xy} = I_{xy} + \overset{\circ}{L}_{\dot{q}} = I_{xy} + \overset{\circ}{M}_{\dot{p}} \tag{10}$$

$$J_{xz} = I_{xz} + \overset{\circ}{N}_{\dot{p}} = I_{xz} + \overset{\circ}{L}_{\dot{r}} \tag{11}$$

$$J_{yz} = I_{yz} + \overset{\circ}{M}_{\dot{r}} = I_{yz} + \overset{\circ}{N}_{\dot{q}} \tag{12}$$

Since the Airship is symmetric about the x-z plane:

$$J_{xy} = J_{yz} = 0 \tag{13}$$

The 6 DOF equations of motion are developed using the Newton-Euler method for each degree of freedom. These equations have been simplified based on the assumed symmetry of a geometrically ideal airship and after some manipulation can be presented in the form of:

$$M\begin{bmatrix} \dot{u} \\ \dot{v} \\ \dot{w} \\ \dot{p} \\ \dot{q} \\ \dot{r} \end{bmatrix} = \begin{array}{l} F_d(u,v,w,p,q,r) + A(u,v,w,p,q,r) + G(\lambda_{31},\lambda_{32},\lambda_{33}) \\ + P(propulsion\ forces\ and\ moments) \end{array} \tag{14}$$

where,

$M =$ 6x6 Mass matrix
$F_d =$ 6x1 matrix Dynamics Force vector
$A =$ 6x1 matrix Aerodynamics vector
$G =$ 6x1 matrix Gravitational and Buoyancy vector
$P =$ 6x1 matrix Propulsion vector

The Mass matrix M including simplifications due to vehicle geometry, is shown below

$$M = \begin{bmatrix} m_x & 0 & 0 & 0 & ma_z - \overset{\circ}{X}_{\dot{q}} & 0 \\ 0 & m_y & 0 & -ma_z - \overset{\circ}{Y}_{\dot{p}} & 0 & ma_x - \overset{\circ}{Y}_{\dot{r}} \\ 0 & 0 & m_z & 0 & -ma_x - \overset{\circ}{Z}_{\dot{q}} & 0 \\ 0 & -ma_z - \overset{\circ}{L}_{\dot{v}} & 0 & J_x & 0 & -J_{xz} \\ ma_z - \overset{\circ}{M}_{\dot{u}} & 0 & -ma_x - \overset{\circ}{M}_{\dot{w}} & 0 & J_y & 0 \\ 0 & ma_x - \overset{\circ}{N}_{\dot{v}} & 0 & -J_{xz} & 0 & J_z \end{bmatrix} \tag{15}$$

The Dynamics Force Vector F_d is shown below with simplifications due to symmetry about the XZ plane.

$$F_d = \begin{bmatrix} f_1 & f_2 & f_3 & f_4 & f_5 \end{bmatrix}^T \tag{16}$$

where,

$$
\begin{aligned}
f_1 &= -m_z wq + m_y rv + m\left[a_x\left(q^2 + r^2\right) - a_z rp\right] \\
f_2 &= -m_x ur + m_z pw + m\left[a_x pq - a_z rq\right] \\
f_3 &= -m_y vp + m_x qu + m\left[-a_x rp + a_z\left(q^2 + p^2\right)\right] \\
f_4 &= -\left(J_z - J_y\right)rq + J_{xz} pq + ma_z\left(ur - pw\right) \\
f_5 &= -\left(J_x - J_z\right)pr + J_{xz}\left(r^2 - p^2\right) + m\left[a_x\left(vp - qu\right) - a_z\left(wq - rv\right)\right] \\
f_6 &= -\left(J_y - J_x\right)qp - J_{xz}\left(qr\right) + m\left[-a_x\left(ur - pw\right)\right]
\end{aligned}
$$

The Aerodynamics Vector A is shown below and its terms are traditionally defined through wind tunnel tests.

$$
A = \begin{bmatrix} A_{X_B} & A_{Y_B} & A_{Z_B} & A_{L_B} & A_{M_B} & A_{N_B} \end{bmatrix}^T \tag{17}
$$

where,

$$
\begin{aligned}
A_X &= \overset{\circ}{X}_\delta\left(\delta_e + \delta_r\right) \\
A_Y &= \overset{\circ}{Y}_\delta \delta_r \\
A_Z &= \overset{\circ}{Z}_\delta \delta_e \\
A_L &= 0 \\
A_M &= \overset{\circ}{M}_\delta \delta_e \\
A_N &= \overset{\circ}{N}_\delta \delta_r
\end{aligned}
$$

Since our linear airship dynamic model is only longitudinal and has a cross-shaped fin orientation at the rear, the rudder control input has no effect on the dynamics. Therefore, all δ_r terms are omitted. The Gravity and Buoyancy vector G is shown below with simplifications due to symmetry about the XZ plane.

$$
G = \begin{bmatrix} \lambda_{31}\left(W - B\right) \\ \lambda_{32}\left(W - B\right) \\ \lambda_{33}\left(W - B\right) \\ -\lambda_{32} a_z W \\ \left(\lambda_{31} a_z - \lambda_{33} a_x\right)W \\ \lambda_{32} a_x W \end{bmatrix} \tag{18}
$$

where,

$$
\begin{aligned}
\lambda_{31}\left(W - B\right) &= -\left(mg - B\right)\sin\left(\theta + \theta_e\right) \\
\lambda_{32}\left(W - B\right) &= \left(mg - B\right)\sin\phi\cos\left(\theta + \theta_e\right) \\
\lambda_{33}\left(W - B\right) &= \left(mg - B\right)\cos\phi\cos\left(\theta + \theta_e\right) \\
-\lambda_{32} a_z W &= -\left(mga_z + Bb_z\right)\sin\phi\cos\left(\theta + \theta_e\right) \\
\left(\lambda_{31} a_z - \lambda_{33} a_x\right)W &= -\left(mga_z + Bb_z\right)\sin\left(\theta + \theta_e\right) - \left(mga_x + Bb_x\right)\cos\phi\cos\left(\theta + \theta_e\right)
\end{aligned}
$$

$$\lambda_{32} a_x W = \left(mga_x + Bb_x\right)\sin\phi\cos\left(\theta + \theta_e\right)$$

The Propulsion vector is defined through the geometry of the airship, and is shown below.

$$P = \begin{bmatrix} X_{prop} & Y_{prop} & Z_{prop} & L_{prop} & M_{prop} & N_{prop} \end{bmatrix}^T \tag{19}$$

where,

$$\begin{aligned}
X_{prop} &= T_s \cos\mu_s + T_p \cos\mu_p \\
Y_{prop} &= 0 \\
Z_{prop} &= -T_s \sin\mu_s - T_p \sin\mu_p \\
L_{prop} &= \left(T_p \sin\mu_p - T_s \sin\mu_s\right) d_y \\
M_{prop} &= T_p\left(d_z \cos\mu_p - d_x \sin\mu_p\right) + T_s\left(d_z \cos\mu_s - d_x \sin\mu_s\right) \\
N_{prop} &= \left(T_p \cos\mu_p - T_s \cos\mu_s\right) d_y
\end{aligned}$$

The assumption is made that thrust is controlled symmetrically and synchronously such that the port and starboard forces are equal[3]. This allows for

$$\begin{aligned}
T_p + T_s &= T_0 \\
\mu_p + \mu_s &= 0 \\
T_p &= T_s
\end{aligned} \tag{20}$$

giving,

$$\begin{aligned}
Y_{prop} &= Z_{prop} = L_{prop} = N_{prop} = 0 \\
X_{prop} &= T_0 \\
M_{prop} &= T_0 d_z
\end{aligned} \tag{21}$$

Using Eq. 14 with the now defined terms, the resulting matrix can be calculated and will be linearized in the next subsection.

B. Linearized Longitudinal State-Space Dynamic Model

In order to linearize the previous equations, small disturbance theory is applied. Small-disturbance theory is discussed in greater detail in Nelson[1]. The assumption that the longitudinal and lateral equations can be decoupled, or separated, is made allowing the longitudinal equations to be developed separately, as presented below. The method used is taken from Khoury and Gillett[3].

Linearized Longitudinal Equations of Motion:

$$m_x\dot{u} + \left(ma_z - \overset{\circ}{X}_{\dot{q}} \right)\dot{q} =$$

$$\left\{ \begin{array}{l} X_e + \overset{\circ}{X}_u u + \overset{\circ}{X}_w w + \left(\overset{\circ}{X}_q - m_z W_e \right) q + \overset{\circ}{X}_\delta \left(\delta_e + \delta_r \right) \\ + \overset{\circ}{X}_t \delta_t + T_e - \left(mg - B \right)\left(\sin\theta_e + \theta\cos\theta_e \right) \end{array} \right\} \tag{22}$$

The linearized axial force equation (Eq. 22) is derived from the nonlinear axial force components in Eq. 14. The aerodynamic, buoyant, gravitational, control surface, and propulsive force contributions have been implemented directly into Eq. 21.

$$m_z\dot{w} - \left(ma_x - \overset{\circ}{Z}_{\dot{q}} \right)\dot{q} =$$

$$\left\{ \begin{array}{l} Z_e + \overset{\circ}{Z}_u u + \overset{\circ}{Z}_w w + \left(\overset{\circ}{Z}_q - m_x U_e \right) q + \overset{\circ}{Z}_\delta \delta_e \\ + \left(mg - B \right)\left(\cos\theta_e - \theta\sin\theta_e \right) \end{array} \right\} \tag{23}$$

The linearized normal force equation (Eq. 23) is derived from the nonlinear normal force components in Eq. 14. The aerodynamic, buoyant, gravitational, control surface, and propulsive force contributions have been implemented directly into Eq. 23

$$J_y\dot{q} + \left(ma_z - \overset{\circ}{M}_{\dot{u}} \right)\dot{u} - \left(ma_x - \overset{\circ}{M}_{\dot{w}} \right)\dot{w} =$$

$$\left\{ \begin{array}{l} M_e + \overset{\circ}{M}_u u + \overset{\circ}{M}_w w + \left(\overset{\circ}{M}_q - ma_x U_e - ma_z W_e \right) q + \overset{\circ}{M}_t \delta_t + \overset{\circ}{M}_\delta \delta_e \\ + T_e d_z - \theta\left\{ \left(mga_z + Bb_z \right)\cos\theta_e - \left(mga_x + Bb_x \right)\sin\theta_e \right\} \\ - \left(mga_z + Bb_z \right)\sin\theta_e - \left(mga_x + Bb_x \right)\cos\theta_e \end{array} \right\} \tag{24}$$

The linearized pitching moment equation (Eq. 24) is derived from the nonlinear pitching moment components in Eq. 14. The aerodynamic, buoyant, gravitational, control surface, and propulsive moment contributions have been implemented directly into Eq. 24. To further simplify the longitudinal equations, trim conditions can be applied. Trim conditions assume that the airship is in equilibrium, causing all perturbation variables to reduce to zero. This assumption results in the following equations.

$$X_e + T_e - (mg - B)\sin\theta_e = 0 \tag{25}$$

$$Z_e + (mg - B)\cos\theta_e = 0 \tag{26}$$

$$M_e + T_e - (mga_z + Bb_z)\sin\theta_e - (mga_x + Bb_x)\cos\theta_e = 0 \tag{27}$$

To satisfy these equations the thrust T_e, buoyancy force B, and center of volume, b_x and b_z are adjusted simultaneously until the left hand side equates to the right hand side. For the model being created, the airship is

trimmed around an operating point defined by level flight at a given altitude, maintaining a constant forward velocity, elevator angle, throttle setting, and vector angle setting. These trim conditions can then be substituted into Eqs. 22, 23, and 24, which is written in state-space form.

$$m\dot{x} = ax + bu \tag{28}$$

where,

$$\bar{x}^T = \begin{bmatrix} u & w & q & \theta \end{bmatrix}$$

$$\bar{u}^T = \begin{bmatrix} \delta_e & \delta_r \end{bmatrix}$$

$$m = \begin{bmatrix} m_x & 0 & \left(ma_z - \mathring{X}_{\dot{q}}\right) & 0 \\ 0 & m_z & -\left(ma_x + \mathring{Z}_{\dot{q}}\right) & 0 \\ \left(ma_z - \mathring{M}_{\dot{u}}\right) & -\left(ma_x + \mathring{M}_{\dot{w}}\right) & J_y & 0 \\ 0 & 0 & 0 & 1 \end{bmatrix}$$

$$b = \begin{bmatrix} \mathring{X}_{\delta_e} & \mathring{X}_{\delta_t} \\ \mathring{Z}_{\delta_e} & \mathring{Z}_{\delta_t} \\ \mathring{M}_{\delta_e} & \mathring{M}_{\delta_t} \\ 0 & 0 \end{bmatrix}$$

$$a = \begin{bmatrix} \mathring{X}_u & \mathring{X}_w & \left(\mathring{X}_q - m_z W_e\right) & -\left(mg - B\right)\cos\theta_e \\ \mathring{Z}_u & \mathring{Z}_w & \left(\mathring{Z}_q + m_x U_e\right) & -\left(mg - B\right)\sin\theta_e \\ \mathring{M}_u & \mathring{M}_w & \left(\mathring{M}_q - ma_x U_e - ma_z W_e\right) & -\left\{\left(mga_z + Bb_z\right)\cos\theta_e - \left(mga_x + Bb_x\right)\sin\theta_e\right\} \\ 0 & 0 & 1 & 0 \end{bmatrix}$$

Using the state form of Eq. 28, both sides can be left multiplied by the inverse of m, giving,

$$\dot{\bar{x}} = A_{4\times4}\bar{x} + B_{4\times2}\bar{u} \tag{29}$$

where,

$$A_{4x4} = m^{-1}a = \begin{bmatrix} x_u & x_w & x_q & x_\theta \\ z_u & z_w & z_q & z_\theta \\ m_u & m_w & m_q & m_\theta \\ 0 & 0 & 1 & 0 \end{bmatrix}$$

$$B_{4x2} = m^{-1}b = \begin{bmatrix} \overset{\circ}{x}_{\delta_e} & \overset{\circ}{x}_{\delta_t} \\ \overset{\circ}{z}_{\delta_e} & \overset{\circ}{z}_{\delta_t} \\ \overset{\circ}{m}_{\delta_e} & \overset{\circ}{m}_{\delta_t} \\ 0 & 0 \end{bmatrix}$$

Now having determined the linear state-space dynamic model, the many terms it contains must be defined. The following explanation will address all terms except for the stability derivatives, which are explained in Section C. Beginning with the mass matrix *m*, which has been reproduced below for convenience, all variables are defined while their respective descriptions are found in the nomenclature section of this paper.

$$m = \begin{bmatrix} m_x & 0 & \left(ma_z - \overset{\circ}{X}_{\dot{q}}\right) & 0 \\ 0 & m_z & -\left(ma_x + \overset{\circ}{Z}_{\dot{q}}\right) & 0 \\ \left(ma_z - \overset{\circ}{M}_{\dot{u}}\right) & -\left(ma_x + \overset{\circ}{M}_{\dot{w}}\right) & J_y & 0 \\ 0 & 0 & 0 & 1 \end{bmatrix} \tag{30}$$

where,

$$\overset{\circ}{X}_{\dot{q}} = 0 \qquad \overset{\circ}{M}_{\dot{u}} = 0$$

$$\overset{\circ}{Z}_{\dot{q}} = 0 \qquad \overset{\circ}{M}_{\dot{w}} = 0$$

The virtual mass and inertia terms above, $\overset{\circ}{X}_{\dot{q}}$, $\overset{\circ}{Z}_{\dot{q}}$, $\overset{\circ}{M}_{\dot{u}}$, and $\overset{\circ}{M}_{\dot{w}}$ have been individually assessed by Gomes who has determined their effects to be negligible[4]. To define the apparent masses (Eqs. 4-6) the values of $\overset{\circ}{X}_{\dot{u}}$ and $\overset{\circ}{Z}_{\dot{w}}$ are found by using the following equations, all of which are found in Sir Horace Lamb's Book "Hydrodynamics"[5].

$$\dot{X}_{\dot{u}} = -k_1 B / g \tag{31}$$

$$\dot{Z}_{\dot{w}} = -k_2 B / g \tag{32}$$

$$\dot{M}_{\dot{q}} = -k'[B / g][\frac{l^2 + d^2}{20}] \tag{33}$$

where,

$$k' = e^4 \frac{\overline{\beta} - \overline{\alpha}}{(2 - e^2)(2e^2 - (2 - e^2)(\overline{\beta} - \overline{\alpha}))}$$

$$k_1 = \frac{\overline{\alpha}}{2-\overline{\alpha}}$$

$$k_2 = \frac{\overline{\beta}}{2-\overline{\beta}}$$

$$\overline{\alpha} = \frac{2(1-e^2)}{e^3(\frac{1}{2}\log\left(\frac{1+e}{1-e}\right)-e)}$$

$$\overline{\beta} = \frac{1}{e^2} - \frac{(1-e^2)}{2e^3(\log\left(\frac{1+e}{1-e}\right))}$$

$$e = \sqrt{1-k\frac{b^2}{a^2}}$$

$$a = \frac{l}{2}$$

$$b = \frac{d}{2}$$

$$B = Vol \cdot \rho \cdot g$$

For reference, $\overset{\circ}{Z}_{\dot{w}} = \overset{\circ}{Y}_{\dot{v}}$ and $\overset{\circ}{M}_{\dot{q}} = \overset{\circ}{N}_{\dot{r}}$. It is important to notice that the virtual mass and inertia nomenclature closely resembles that of the stability derivatives. These two should not be confused, as $\overset{\circ}{X}_{\dot{u}} \neq \overset{\circ}{X}_u$; virtual terms are identified by a dot over the subscripted character.

V. The Common "a" Method of Airship Modeling

The stability derivatives used to generate the linear model are obtained from Nelson[1]. These are used to further define the *a* matrix seen in Eq. 28**,** which is also reproduced below for convenience.

$$a = \begin{bmatrix} \overset{\circ}{X}_u & \overset{\circ}{X}_w & \left(\overset{\circ}{X}_q - m_z W_e\right) & -(mg-B)\cos\theta_e \\ \overset{\circ}{Z}_u & \overset{\circ}{Z}_w & \left(\overset{\circ}{Z}_q + m_x U_e\right) & -(mg-B)\sin\theta_e \\ \overset{\circ}{M}_u & \overset{\circ}{M}_w & \left(\overset{\circ}{M}_q - ma_x U_e - ma_z W_e\right) & -\{(mga_z + Bb_z)\cos\theta_e - (mga_x + Bb_x)\sin\theta_e\} \\ 0 & 0 & 1 & 0 \end{bmatrix} \quad (34)$$

where,

$$\overset{\circ}{X}_u = \frac{-(C_{D_u} + 2C_{D_0})QS}{U_e}$$

$$\overset{\circ}{X}_w = \frac{-(C_{D_\alpha} - C_{L_0})QS}{U_e}$$

$$\overset{\circ}{X}_q = 0$$

$$\overset{\circ}{Z}_u = \frac{-(C_{L_u} + 2C_{L_0})QS}{U_e}$$

$$\overset{\circ}{Z}_w = \frac{-(C_{L_\alpha} + 2C_{D_0})QS}{U_e}$$

$$\overset{\circ}{Z}_q = C_{Z_q}\frac{QS\overline{c}}{2U_e}$$

$$\overset{\circ}{M}_u = C_{m_u}\frac{QS\overline{c}}{U_e}$$

$$\overset{\circ}{M}_w = C_{m_\alpha}\frac{QS\overline{c}}{2U_e}$$

$$\overset{\circ}{M}_q = C_{m_q}\frac{QS\overline{c}^2}{2U_e}$$

The mass terms in the aircraft stability derivatives are omitted in order to insert the airship mass terms. This happens when the aircraft *a* matrix is multiplied by the inverse mass matrix of the airship. Common to most of the above derivatives are Q, S, and $\bar{c}$. Assumptions made for S and $\bar{c}$ are found in the next section, whereas Q is defined below.

$$Q = \frac{1}{2}\rho U_e^{\ 2} \tag{35}$$

A. Implementing Stability Derivatives into the Linearized Longitudinal State-Space Dynamic Model

In order to employ the stability derivatives in the state-space dynamic model, certain assumptions had to be made. These assumptions came from various sources and previous work and are validated below.

The following longitudinal stability coefficients, while originally based off of an aircraft, are based on Gomes' flight dynamics thesis[4]. C_{D_0}, C_{D_α}, C_{L_0}, C_{L_α}, C_{m_u}, and C_{m_α} were determined using Gomes' work, C_{D_u} is found in Nelson[1], and $C_{L_{\alpha_t}}$ and $C_{m_{\delta_e}}$ are estimated through XFOIL 2D code and Prandtl lifting line theory, respectively.

The remaining longitudinal stability coefficients can be derived from equations involving the physical parameters of the ship[1].

$$C_{L_u} = \frac{M_a^{\ 2}}{1 - M_a^{\ 2}} C_L \tag{36}$$

$$C_{Z_q} = -2\eta C_{L_{\alpha_t}} V_H \tag{37}$$

$$C_{m_q} = \frac{C_{Z_q} l_t}{\bar{c}} \tag{38}$$

$$C_{Z_{\delta_e}} = -C_{L_{\alpha_t}} \tau \frac{S_t}{S} \eta \tag{39}$$

where,

$$V_H = \frac{S_t}{S}\frac{l_t}{\bar{c}}$$

The value for C_{L_u} is estimated to be zero, since the Mach number is very small at low speeds. τ is found by using Figure 2.21 in Nelson[1]. η is estimated between the values of 0.8 and 1.2 for different configurations of the tail.

The stability derivative $\mathring{X}_q$ was set to zero as its effects have been found to be negligible through varying its value and comparing the system responses. The following estimations were also made,

$$S = Vol^{2/3} \tag{40}$$

$$\bar{c} = Vol^{1/3} \tag{41}$$

Where $Vol^{2/3}$ has been estimated as the surface area of the lifting surface for the airship, and $Vol^{1/3}$ has been estimated as the mean aerodynamic chord for the airship.

The *b* matrix which has been reproduced below for convenience is characterized by changes in the elevator angle and thrust with respect to forces in the X and Z directions and the pitching moment. The formulas defining select variables are found in Nelson[1]:

$$b = \begin{bmatrix} \mathring{X}_{\delta_e} & \mathring{X}_{\delta_t} \\ \mathring{Z}_{\delta_e} & \mathring{Z}_{\delta_t} \\ \mathring{M}_{\delta_e} & \mathring{M}_{\delta_t} \\ 0 & 0 \end{bmatrix} \tag{42}$$

where,

$$\mathring{Z}_{\delta_e} = C_{Z_{\delta_e}} QS \qquad \mathring{M}_{\delta_e} = C_{m_{\delta_e}} QS\bar{c}$$

$\mathring{X}_{\delta_e}$, $\mathring{X}_{\delta_t}$, $\mathring{Z}_{\delta_t}$, and $\mathring{M}_{\delta_t}$ control inputs are estimated based on other airship models in literature. The values are scaled based on the operating point and trim conditions of the linear model.

In summary, the mass-dependent matrix a in (34), which is used extensively in the airship literature[3], can be populated by stability derivative expressions found in the aircraft literature, This connection between the airship and aircraft literatures is new, and is denoted here as the common "a" method of airship modeling.

VI. Model Validation and Analysis

The common "a" method of airship modeling is validated by comparing it to the linear airship models in the literature. A unit analysis is performed, the eigenvalues/characteristic roots are determined and compared to those of a stable system, and rectangular pulse and doublet responses of the model are compared to that of a known stable system.

All computations and simulations were completed with Simulink inside of MatLab version 7.4.0[16]. To validate the feasibility of using the aircraft formulas with the airship method, the *a* matrices (with mass and inertia) of the two are compared. The airship dynamics *a* matrix[3] is compared to the aircraft dynamics *a* matrix[1], and all of the aircraft variables are found in the same place in the airship matrix, except that the airship matrix has additional variables due to virtual terms.

A. Dimensional Analysis

A dimensional analysis is performed to ensure that the linear longitudinal airship model's *a* matrix had the same units as the linear longitudinal aircraft *a* matrix since this is the matrix used to determine the stability of the system. There are additional virtual mass and inertia terms in the airship matrices, and the dimensional analysis of the two air vehicles shows that the additional terms do not alter the dimensions. The analysis begins with the state-space equation (Eq. 29) below.

$$\dot{\bar{x}} = A_{4\times4}\bar{x} + B_{4\times2}\bar{u} \tag{43}$$

where,

$$\bar{x} = \begin{bmatrix} u \\ w \\ q \\ \theta \end{bmatrix}$$

$$\bar{u} = \begin{bmatrix} \delta_e \\ \delta_t \end{bmatrix}$$

Representing the dimensions of a variable will be achieved using the syntax $\dim(x)$, where x is the variable that will have its dimensions displayed. The dimensions of $\dot{\bar{x}}$ are shown below.

$$\dim(\dot{\bar{x}}) = \begin{bmatrix} m/s^2 \\ m/s^2 \\ rad/s^2 \\ rad/s \end{bmatrix} \tag{44}$$

Both the aircraft and the airship have the same state space derivative state vector $\dot{\bar{x}}$ describing their motion, and the following will show that the derivative state vector $\dot{\bar{x}}$ of both the aircraft and airship have the same dimensions. In both equations the *x* state vector and outputs of longitudinal airship and aircraft models have the same dimensions, showing that the dimensions of the *A* matrix of both the aircraft and the airship are similar will suffice. Beginning with the aircraft,

$$A_{aircraft} = m_{aircraft}^{-1} a_{aircraft} \tag{45}$$

where,

$$A_{aircraft} = Aircraft\ A\ Matrix$$

$$m_{aircraft} = Aircraft\ Mass\ Matrix = \begin{bmatrix} m & 0 & 0 & 0 \\ 0 & m & 0 & 0 \\ 0 & 0 & I_{yy} & 0 \\ 0 & 0 & 0 & 1 \end{bmatrix}$$

$$A_{aircraft} = Aircraft\ A\ Matrix = \begin{bmatrix} \mathring{X}_u & \mathring{X}_w & 0 & -g \\ \mathring{Z}_u & \mathring{Z}_w & u_0 & 0 \\ \mathring{M}_\delta + \mathring{M}_{\dot{w}} Z_u & \mathring{M}_w + \mathring{M}_{\dot{w}} Z_w & \mathring{M}_q + \mathring{M}_{\dot{w}} u_0 & 0 \\ 0 & 0 & 1 & 0 \end{bmatrix}$$

The units of the aircraft mass matrix are:

$$\dim(m_{aircraft}) = \begin{bmatrix} kg & 0 & 0 \\ 0 & kg & 0 \\ 0 & 0 & kgm^2 \end{bmatrix} \tag{46}$$

Since pitch angle (θ) is the integral of pitch rate (q) in the linearized approximation, only the three primary states are considered for this dimensional analysis. Thus, last row and column of the aircraft mass matrix are omitted. The same logic is applied to the aircraft *a* matrix.

The units of the Aircraft *a* matrix are:

$$\dim\left(a_{aircraft}\right)=\begin{bmatrix} \frac{kg}{s} & \frac{kg}{s} & \frac{kgm}{s} \\ \frac{kg}{s} & \frac{kg}{s} & \frac{kgm}{s} \\ \frac{kgm}{s} & \frac{kgm}{s} & \frac{kgm^2}{s} \end{bmatrix} \tag{47}$$

Using Eq. 45 and taking the dimensions of each term,

$$\dim\left(A_{aircraft}\right)=\dim(m_{aircraft}{}^{-1})\dim(a_{aircraft}) \tag{48}$$

$$\dim\left(A_{aircraft}\right)=\begin{bmatrix} \frac{1}{s} & \frac{1}{s} & \frac{m}{s} \\ \frac{1}{s} & \frac{1}{s} & \frac{m}{s} \\ \frac{1}{m\cdot s} & \frac{1}{m\cdot s} & \frac{1}{s} \end{bmatrix} \tag{49}$$

The dimensions of the $A_{aircraft}$ dynamics matrix (mass-less) are now known and the dimensions of $A_{aircraft}\times\overline{x}$ are equal to those in Eq. 44. Working from the other direction, the $A_{airship}$ dynamics matrix is described.

$$A_{airship}=m_{airship}{}^{-1}a_{airship} \tag{50}$$

where,

$$A_{airship}=Airship\ A\ Matrix$$

$$m_{airship}=Airship\ Mass\ Matrix=\begin{bmatrix} m_x & 0 & \left(ma_z-\mathring{X}_{\dot{q}}\right) & 0 \\ 0 & m_z & -\left(ma_x+\mathring{Z}_{\dot{q}}\right) & 0 \\ \left(ma_z-\mathring{M}_{\dot{u}}\right) & -\left(ma_x+\mathring{M}_{\dot{w}}\right) & J_y & 0 \\ 0 & 0 & 0 & 1 \end{bmatrix}$$

$$a_{airship}=Airship\ a\ Matrix=\begin{bmatrix} \mathring{X}_u & \mathring{X}_w & \left(\mathring{X}_q-m_zW_e\right) & -(mg-B)\cos\theta_e \\ \mathring{Z}_u & \mathring{Z}_w & \left(\mathring{Z}_q+m_xU_e\right) & -(mg-B)\sin\theta_e \\ \mathring{M}_u & \mathring{M}_w & \left(\mathring{M}_q-ma_xU_e-ma_zW_e\right) & -\left\{\begin{matrix}(mga_z+Bb_z)\cos\theta_e- \\ (mga_x+Bb_x)\sin\theta_e\end{matrix}\right\} \\ 0 & 0 & 1 & 0 \end{bmatrix}$$

The units of the airship mass matrix are:

$$\dim\left(m_{airship}\right)=\begin{bmatrix} kg & 0 & kgm \\ 0 & kg & kgm \\ kgm & kgm & kgm^2 \end{bmatrix} \tag{51}$$

The last row and column of the airship mass matrix are omitted because the 4th state in the longitudinal state vector is simply the integration of the 3rd state over time. Since pitch angle (θ) is the integral of pitch rate (q), only the three primary states are considered for this dimensional analysis.

Since the dimensions of the $A_{aircraft}$ matrix is known, using the aircraft A matrix in Eq. 45 instead of $A_{airship}$ should yield the same dimensions for $a_{airship}$ as in Eq. 47. By left multiplying Eq. 50 by $m_{airship}$, the following results:

$$m_{airship} \cdot A_{airship} = a_{airship} \tag{52}$$

Now substituting in $A_{aircraft}$ for $A_{airship}$ and taking the dimensions of each term:

$$\dim(m_{airship}) \cdot \dim\left(A_{aircraft}\right) = \dim(a_{airship}) \tag{53}$$

giving,

$$\dim(a_{airship}) = \begin{bmatrix} kg & 0 & kgm \\ 0 & kg & kgm \\ kgm & kgm & kgm^2 \end{bmatrix} \bullet \begin{bmatrix} \frac{1}{s} & \frac{1}{s} & \frac{m}{s} \\ \frac{1}{s} & \frac{1}{s} & \frac{m}{s} \\ \frac{1}{m \cdot s} & \frac{1}{m \cdot s} & \frac{1}{s} \end{bmatrix} = \begin{bmatrix} \frac{2kg}{s} & \frac{2kg}{s} & \frac{2kgm}{s} \\ \frac{2kg}{s} & \frac{2kg}{s} & \frac{2kgm}{s} \\ \frac{3kgm}{s} & \frac{3kgm}{s} & \frac{3kgm^2}{s} \end{bmatrix} \tag{54}$$

Comparing (47) and (54) it is seen that,

$$\dim(a_{airship}) \approx \dim(a_{aircraft}) \tag{55}$$

in the sense that,

$$\begin{bmatrix} \frac{2kg}{s} & \frac{2kg}{s} & \frac{2kgm}{s} \\ \frac{2kg}{s} & \frac{2kg}{s} & \frac{2kgm}{s} \\ \frac{3kgm}{s} & \frac{3kgm}{s} & \frac{3kgm^2}{s} \end{bmatrix} \approx \begin{bmatrix} \frac{kg}{s} & \frac{kg}{s} & \frac{kgm}{s} \\ \frac{kg}{s} & \frac{kg}{s} & \frac{kgm}{s} \\ \frac{kgm}{s} & \frac{kgm}{s} & \frac{kgm^2}{s} \end{bmatrix}$$

The only difference between these two unit analysis matrices is in the numerical coefficients (2 and 3 vs. 1) that scale the matrix elements. This result suggests that the airship a matrix simply has more non-zero elements than the strictly diagonal form of an aircraft mass matrix. Since multiple contributions of similar terms do not effect the dimensional units of the matrix elements, the aircraft and airship have similar a matrices, and it follows that the aircraft and airship have state vectors with the same dimensions, justifying the use of aircraft stability derivatives to determine the $A_{airship}$ matrix.

B. Eigenvalue/Characteristic Root Comparison

The second check was performed by comparing the eigenvalues of the JPL Aerobot linear dynamic model to existing airship models in the literature. Table 1 summarizes the trim parameters and the main physical attributes of the three airships being compared: Gomes' YEZ-2A airship, the Aurora airship, and the JPL Aerobot airship.

Table 1: Geometric Comparison of the YEZ-2A, Aurora, and JPL Aerobot Model

	Length (m)	Diameter (m)	Mass (kg)	Trim Velocity (m/s)
YEZ-2A	129.5	32	86816	5
Aurora Airship	9	3	20	7.5
JPL Aerobot Model	11.43	2.4384	42.5	2

The *A* matrix of the Aurora airship[8] was used as a comparison since it closely resembles the JPL Aerobot, and eigenvalues were taken from Gomes' work for the YEZ-2A airship. The eigenvalues of the Aurora test data, the YEZ-2A data, and our model are compared in Table 2 below.

Table 2: Eigenvalue Comparison of the YEZ-2A, Aurora, and JPL Aerobot Model

Mode	YEZ-2A[4]	Aurora Airship[8]	JPL Aerobot Model
Surge	-0.00565	-0.1426	-0.1198
Heave	-0.0392	-3.7819	-0.1971
Pendulum Oscillation	-0.108 ± 0.264i	-0.2838 ± 0.3182i	-0.0140 ± 0.0636i

By studying Table 2 it can be seen that all sets of eigenvalues are negative and since negative roots describe a stable system, all systems are stable. Furthermore, the fact that all models have two negative real roots and two negative imaginary roots validates our model.

The JPL Aerobot airship model exhibits the surge, heave, and pendulum oscillation modes, which are specific to airships. Aircraft have two sets of complex poles that characterize the phugoid and short period modes. From the eigenvalues for the JPL Aerobot model in Table 2, it is clearly shown that by using aircraft stability derivative estimation techniques from Nelson[1], it is possible to develop an airship dynamic model that responds correctly and exhibits the correct modal behavior. The previous work and information sources that contributed to the development of this linear dynamic modeling method for airships is summarized in Figure 2.

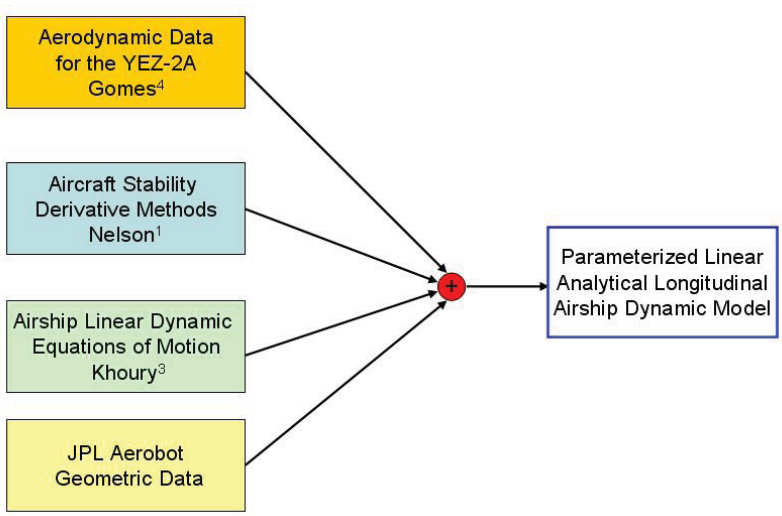

Figure 2: Block Diagram showing the major information sources that contributed to the development of the JPL Aerobot Linear Dynamic Model

C. Model Response Comparison

To compare our JPL Aerobot model with models from the literature, a Simulink model was created to easily generate rectangular pulses and doublet pulses. The open-loop responses from the inputs were plotted using the Matlab. The Simulink model was run using a variable step Matlab ODE45 integrator and graphs were created that compared the YEZ-2A airship data to our parameterized data. These two graphs are explained in more detail below.

1. Rectangular Pulse Response

The YEZ-2A longitudinal model applies a rectangular pulse of -10 degrees for 10 seconds to the airship simulation, and collects data for 20 seconds. These results are shown graphed below in Figure 3 alongside the response of the JPL Aerobot parameterized longitudinal linear airship model.

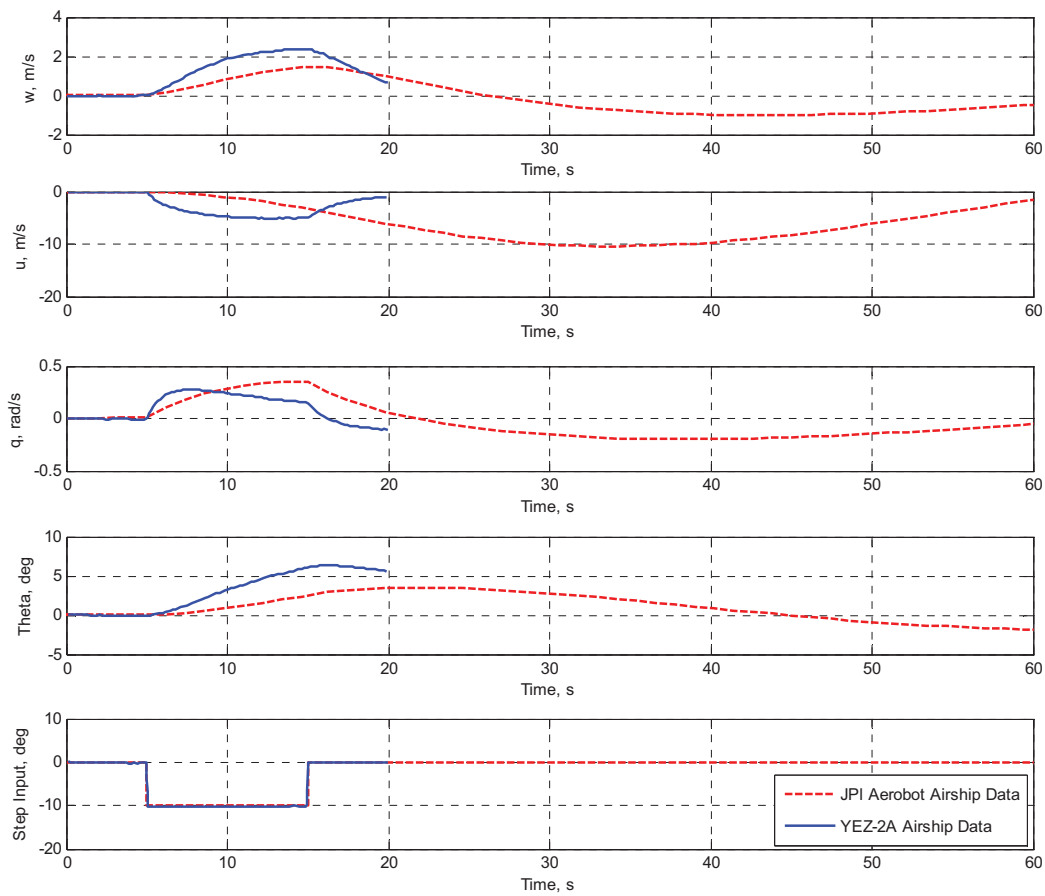

Figure 3: Rectangular Pulse Excitation Response. The YEZ-2A data "u" and "q" data was scaled up by a factor of 20 for plot comparison.

Parts of YEZ-2A data have been amplitude scaled to enable the responses of the systems to be easily compared. By looking at the data, it is observed that the response of the JPL Aerobot model has the same shape as YEZ-2A airship model, except that it reacts slower. All peaks and valleys observed in YEZ-2A airship model data are observed in the JPL Aerobot model, reinforcing our models validity.

2. Doublet Excitation Response

The YEZ-2A dynamic airship model applies a doublet pulse of -15 to 15 degrees over 20 seconds to the model airship, and collects data for 200 seconds. These results are shown graphed below in Figure 4 alongside the response of our parameterized longitudinal linear model.

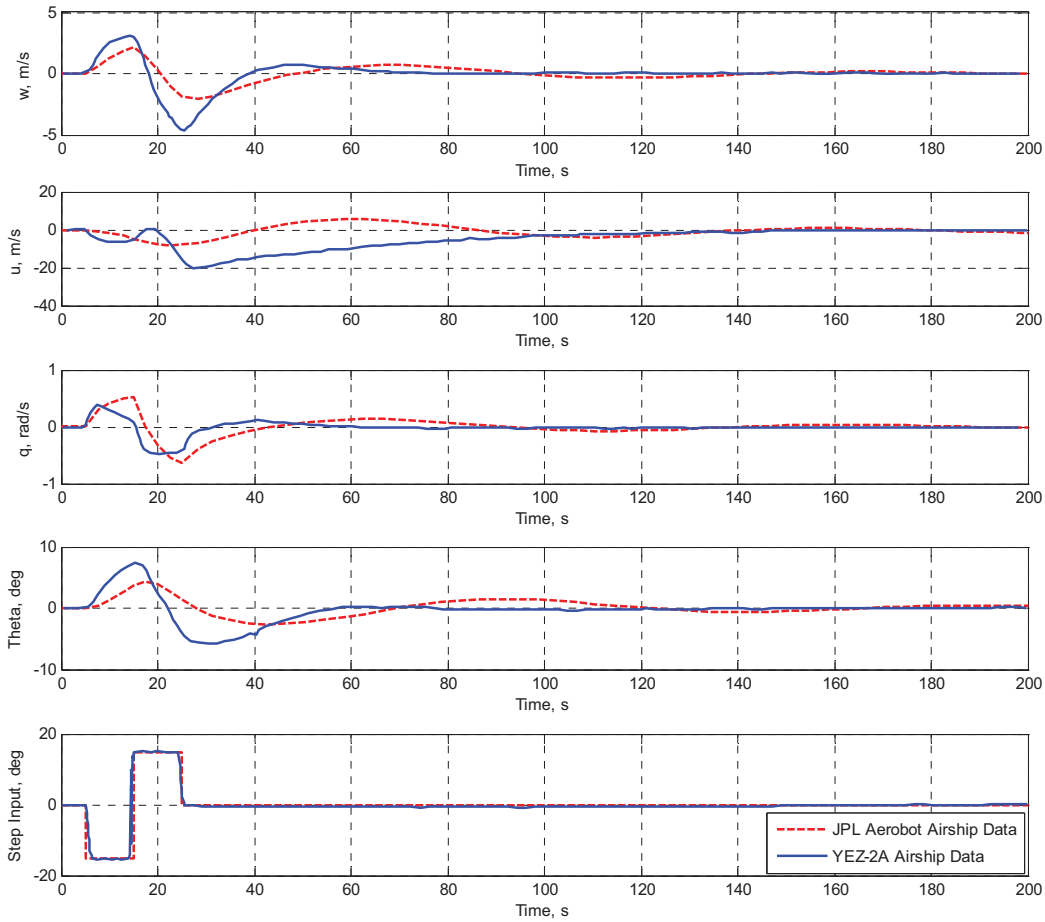

Figure 4: Doublet Excitation Response. The YEZ-2A data "u" and "q" data was scaled up by a factor of 20 for plot comparison.

Parts of the YEZ-2A data have been scaled to enable the responses of the systems to be easily compared. By looking at the data, it is observed that the response of the JPL Aerobot has the same shape as YEZ-2A airship, at times stabilizing around the same time as YEZ-2A data. In the graphs for vertical velocity (w) and pitch angle (θ), our model had a lower amplitude. Again, all peaks and valleys observed in YEZ-2A data are observed in our model, reinforcing our model's validity.

VI. Conclusion

A new technique, denoted as the Common "a" method, is introduced for developing a stable parameterized linear longitudinal dynamic model of an airship. The main idea is to combine classical aircraft stability derivative methods with linear dynamic airship modeling theory. The significance of this is that it does not require any system identification to create a linear model, circumventing the expensive and laborious task of performing extensive flight experiments. The JPL Aerobot model has been validated by dimensional unit analysis, characteristic roots, and response to control input rectangular pulses and doublets. As desired, the JPL Aerobot linear longitudinal airship model produces responses similar to known airship models in the literature. To continue this research, a lateral linear dynamic model is under development using the same methods. Once this is complete, a fully parameterized linear airship dynamic model can be tuned by using flight data from the JPL Aerobot. This complete linear model

can then be used in waypoint navigation, path planning, and autonomous airship control about a specific operating point. The linear model can be tuned easily for trim about additional operating points allowing for the development of a gain scheduling control system. Looking past these milestones, this model will help enable an airship to navigate through the atmosphere of Titan while providing a platform for scientific exploration and experimentation.

Acknowledgments

This work was made possible by the contributions of Daniel Clouse, Arin Morfopoulos, and Jeffery L. Hall, the Aerobot Task Lead. The research described in this paper was performed at the Jet Propulsion Laboratory, California Institute of Technology, under a contract with the National Aeronautics and Space Administration (NASA), and administered through the Intelligent Space (IS) Program. The view and conclusions contained in this document are those of the authors and should not be interpreted as representing the official policies, either expressed or implied, of the sponsoring organizations.

References

[1]Nelson, R.C., *Flight Stability and Automatic Control,* 2nd ed., McGraw-Hill Companies, United States, 1998, Chaps. 3, 4.

[2]Elfes, A., Montgomery, J. F., Hall, J. L., Joshi, S. S., Payne, J., and Bergh, C. F., "Autonomous Flight Control for a Planetary Exploration Aerobot", *AIAA Space 2005 Conference*, Long Beach, CA, Aug 30 – Sept 1, AIAA Paper 2005-6717.

[3]Khoury, G., and Gillet, D., *Airship Technology*, Cambridge University Press, UK, February 1999.

[4]Gomes, S.B.V , "An Investigation on the Flight Dynamics of Airships with Application to the YEZ-2A," Ph.D Thesis, College of Aeronautics, Cranfield University, October 1990.

[5]Lamb, H. Sir., M.A., LL.D., Sc.D., F.R.S., *Hydrodynamics*, 6th ed., Dover Publications, New York, 1945, pp. 153-155.

[6]"Solar System Exploraion Roadmap for NASA's Science Mission Directorate," JPL D-35618, Huly 2006.

[7]Kerzhanovich, V. V., Cutts, J. A., Cooper, H. W., Hall, J. L., et al. "Breakthrough in Mars Balloon Technology", *Proceeding of the World Space Congress / 34th Scientific Assembly of the Committee on Space Research* (COSPAR), Houston, TX, USA, October, 2002.

[8]Cortés, V. R., Azinheira, J. R., Paiva, E. C., Faria, B., Ramos, J., Bueno, S., "Experimental Identification of Aurora Airship", *IAV 2004*, Lisbon, Jul 2004.

[9]DeLaurier, J. D. and Schenk, D., "Airship Dynamic Stability", *AIAA Lighter-Than-Air Systems Technology Conference*, 3rd, Rickey's Hyatt House, Palo Alto, CA, July 11-13, 1979, AIAA Paper 79-1591.

[10]Lowe, J. D. and DeLaurier, J. D., "A Six-Degree of Freedom Heavy Lift Airship Flight Simulation", *AIAA Lighter-Than-Air Systems Technology Conference*, 5th, Anaheim, CA, July 25-27, 1983, AIAA Paper 83-1988.

[11] Elfes, A., Hall, J., Montgomery, J., Bergh, C., and Dudik, B., "Towards a Substantially Autonomous Aerobot for Titan Exploration," *AIAA's 3rd Annual Aviation Technology, Integration, and Operations (ATIO) Technology Conference*, Denver, CO; November 17-19, 2003, AIAA Paper 2003-6714.

[12] Tischler, M. B., and Remple, R. K., *Aircraft and Rotorcraft System Identification: Engineering Methods with Flight Test Exmaples*, AIAA Education Series, AIAA, Reston, Virginia, 2006.

[13]Elfes, A., Hall, J., Kulczycki, E., Morfopoulos, A., Montgomery, J., Clouse, D., Bayard, D., Cameron, J., Machuzak, R., Magnone, L., Bergh, C., and Walsh, G., "Autonomy Capability Development for a Titan Aerobot*," Fourth Annual International Planetary Probe Workshop (IPPW-4)*, Pasadena, CA, June 2006.

[14]Joshi, S., Acosta, D., Payne, J., and Sharma S., Elfes, A., Trebi-Ollennu, A., and Hall, J., "Dynamics and Control Study of Titan Aerobot from a Systems Design Perspective," *AIAA Guidance, Navigation, and Control Conference and Exhibit*, San Francisco, California, Aug. 15-18, 2005, AIAA-2005-5975.

[15]Kampke, T., Elfes, A., "Optimal Wind Assisted Flight Planning for Planetary Aerobots," *Proceeding of 2004 IEEE International Conference on Robotics and Automation* (ICRA), New Orleans, LA, April 2004.

[16] Dabney, J.B., and Harman, T.L., *Mastering Simulink*, Prentice Hall, United States, 2003